INSTITUTE OF PHYSICS PUBLISHING JOURNAL OF OPTICS B: QUANTUM AND SEMICLASSICAL OPTICS

J. Opt. B: Quantum Semiclass. Opt. **4** (2002) 326–335 PII: S1464-4266(02)36456-5

Temperature-enhanced squeezing in cavity QED

D Spehner[1] **and M Orszag**[2]

[1] Universität Essen, Fachbereich Physik, D-45117 Essen, Germany
[2] Pontificia Universidad Católica de Chile, Facultad de Física, Casilla 306, Santiago 22, Chile

Received 25 April 2002, in final form 1 August 2002
Published 29 August 2002
Online at stacks.iop.org/JOptB/4/326

Abstract
We study the time evolution of the quantum field inside a cavity coupled to a beam of two-level atoms of temperature T, given that each atom, after having crossed the cavity, interacts with a classical field $\mathcal{E}$ and finally with a detector measuring its state. It is found that, if the coupling between the atoms and the quantum field is weak and $\mathcal{E}$ is not too small, for any given realization of the measurements, an arbitrary initial state of the field localizes after some time into squeezed states. The centre α of the squeezed state moves randomly in time in the complex plane, but the squeezing amplitude r and phase ϕ show very small fluctuations. Their mean values $\overline{r}$ and $\overline{\phi}$ are independent of the random results of the measurements, of the initial state and of the atom–field coupling constant λ. The time evolution of r and ϕ is determined analytically by deriving and solving the quantum state diffusion equation describing the field dynamics in the limit of small λ, keeping $\mathcal{E}$ finite. It is shown that $\overline{r}$ increases with T, i.e., the squeezing is enhanced by increasing the temperature of the atomic beam.

Keywords: Open quantum systems, quantum trajectories, micromasers

1. Introduction

Dissipation has played a central role in quantum optics. A typical example of this is spontaneous emission, where an individual atom is coupled to an ensemble of modes of the electromagnetic field, giving, as a final result, a finite lifetime to every atomic excited state. Traditionally, the dynamics of a dissipative quantum system is described through a master equation for the reduced density matrix, obtained by tracing out the degrees of freedom of the reservoir (the electromagnetic field in the above example) and making the Markov approximation. Also, a great deal of work has been done in quantum optics on continuously monitored systems with dissipation, referred to as 'quantum jumps' or 'Monte Carlo wavefunction' schemes, which are examples of a wider class of techniques concerned with 'quantum trajectories'. In these approaches, the master equation is replaced by a stochastic differential equation for a pure state. If one averages over the realizations of the dynamical noise, the master equation is reproduced. Such a stochastic equation is referred to as the 'unraveling' of the master equation. This is not a unique process and there can be several stochastic equations that will average to the same master equation [1–12]. This technique has become important, because the trend in modern optics has been towards isolating and manipulating individual quantum systems. Examples include cavity QED with single atoms and photons [13], micromasers [14, 15], microlasers [16], trapped ions cooled to the motional zero point [17], Coulomb blockade [18] and Bose–Einstein condensates in electromagnetic traps [19]. Wide interest in such systems has been stimulated by possible applications to quantum computers (manipulation and storage of quantum states).

The aim of this paper is to investigate the localization properties of quantum trajectories for the electromagnetic field inside a high-Q cavity interacting with a beam of two-level atoms, which form the reservoir of temperature T. The states of the atoms leaving the cavity are measured by a detector. A laser field $\mathcal{E}$ with frequency close to the resonance with the atomic transition is placed between the cavity and the detector. The same system has been considered in [20] in the reverse situation where one knows exactly the state of each atom before it crosses the cavity and no measurement is performed on it at its exit (its final state being thus unknown). It has been shown in this reference that the cavity field evolves at large

times to a state which is completely controlled by the initial states of the atoms, and that any field state can be obtained asymptotically by an appropriate choice of the sequence of atomic states. We find in our case a somewhat related result: for sufficiently large $\mathcal{E}$ and small atom–field coupling, the cavity field evolves at large times to squeezed states $|\alpha, \xi\rangle$, whose squeezing parameters $r = |\xi|$ and $\phi = \arg(\xi)/2$ are controlled by the temperature T of the beam and by $\mathcal{E}$, respectively. An important difference is, however, that randomness is left in the problem: the centre α fluctuates randomly in the complex plane, in such a way that the photon number distribution reproduces after time averaging the equilibrium (Bose–Einstein) distribution at temperature T. The present work extends some previous results presented in [21].

2. The experimental scheme

Let us consider one mode of the quantized electromagnetic field of a lossless cavity coupled to its environment. The environment is a beam of atoms prepared in one of two Rydberg states $|g\rangle$ ('ground state') and $|e\rangle$ ('excited state') in resonance with the frequency ω of the mode. The fluxes r_g and r_e of atoms crossing the cavity, prepared respectively in states $|g\rangle$ and $|e\rangle$, are assumed to be such that at most one atom is in the cavity at any time. The time interval between the crossing of consecutive atoms is $\delta t = (r_g + r_e)^{-1}$. To simplify, all the atoms of the beam are supposed to have the same speed. They thus spend the same time $\tau < \delta t$ in the cavity, interacting with the photon mode. The atom–mode interaction Hamiltonian is in the interaction picture (rotating-wave approximation) [22]

$$H_{\rm int} = -{\rm i}(\lambda^* |g\rangle\langle e| a^\dagger - \lambda |e\rangle\langle g| a), \tag{1}$$

where $a^\dagger$ and a are the creation and annihilation operators of a photon in the cavity mode. The coupling constant λ is equal to $\sqrt{q^2\omega/2\varepsilon_0 V}\,\vec{d}_{ge}\cdot\vec{\sigma}$, where $\vec{d}_{ge}$ is the matrix element of the atomic dipole, $\vec{\sigma}$ the polarization vector of the mode, q the charge of the electron and V the volume of the cavity.

At the exit of the cavity, the atoms enter into a second cavity, identical to the first but containing a classical field $\mathcal{E}$ (figure 1). We again assume that each atom spends the same time $\tau_L < \delta t$ there, and denote by $U = {\rm e}^{-{\rm i}\tau_L H_L}$ the time evolution operator of the atom driven by the classical field. In the special case of a classical laser field $\vec{\mathcal{E}}$, the atom–classical field interaction Hamiltonian reads

$$H_L = -\frac{\rm i}{2}(\Omega^* |g\rangle\langle e| - \Omega |e\rangle\langle g|) - \delta |e\rangle\langle e|, \tag{2}$$

where $\Omega = {\rm i}\vec{d}_{ge}\cdot\vec{\mathcal{E}}$ is the Rabi frequency and $\delta = \omega_L - \omega$ is the detuning between the laser and the atomic frequencies.

Finally, the state of each atom is measured at the exit of the second cavity by a perfect detector, telling us whether it is in its ground or its excited state. The corresponding experimental set-up is presented in figure 1. It has been considered in [23] without the second cavity. A similar set-up has been studied in [24], but the atoms were assumed to be pumped in their 'excited' state before entering the first cavity ($r_g = 0$). In contrast, we shall assume in what follows $r_g > r_e$. The times of flight of the atoms between the two cavities and between the second cavity and the detector are supposed to be much smaller than the lifetime of $|e\rangle$, so spontaneous emission of photons can be neglected.

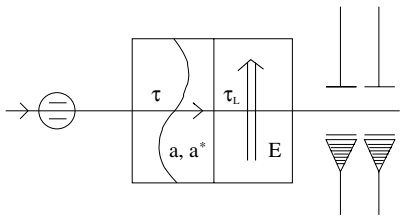

Figure 1. The two-level atoms of the beam cross one by one a cavity containing the quantum field studied, a, a second cavity containing a laser field $\mathcal{E}$ and a detector measuring their states.

3. Stochastic dynamics of the quantum field

Let us determine the evolution of the state of the field in the first cavity when one atom, initially in state $|i\rangle$, $i = g$ or e, crosses the two cavities and the detector. At the time t just prior the entrance of the atom in the first cavity, the wavefunction $|\Psi(t)\rangle$ of the total system 'atom + quantum field' is a tensor product state $|\Psi(t)\rangle = |i\rangle|\psi(t)\rangle$. Since the two fields are in separated cavities, the atom interacts with the quantum field *before* interacting with the classical field $\mathcal{E}$. The total wavefunction at the exit of the second cavity (before the measurement) is thus in the interaction picture

$$|\Psi_{\rm ent}\rangle = {\rm e}^{-{\rm i}\tau_L H_L}{\rm e}^{-{\rm i}\tau H_{\rm int}}|\Psi(t)\rangle. \tag{3}$$

The interaction leads to an entanglement between the quantum field and the atom, i.e., $|\Psi_{\rm ent}\rangle$ is no longer a tensor product state. After the measurement on the atom has been performed, the field and the atom become again disentangled and the wavefunction of the total system is

$$\begin{aligned} |\Psi(t+\delta t)\rangle &= |j\rangle|\psi(t+\delta t)\rangle, \\ |\psi(t+\delta t)\rangle &= \frac{\langle j|\Psi_{\rm ent}\rangle}{\|\langle j|\Psi_{\rm ent}\rangle\|}, \end{aligned} \tag{4}$$

with $j = g$ if the atom is detected in state $|g\rangle$ and $j = e$ if it is detected in state $|e\rangle$. It is convenient to introduce the complex numbers

$$\eta = \lambda\tau, \qquad \epsilon = \frac{u_{eg}}{\lambda\tau u_{ee}} = -\frac{u_{ge}^*}{\lambda\tau u_{gg}^*} \tag{5}$$

and the operator

$$\tilde{a} = a\,{\rm sinc}(|\eta| n^{\frac{1}{2}}), \tag{6}$$

where $u_{ij} = \langle i|{\rm e}^{-{\rm i}\tau_L H_L}|j\rangle$, $n^{1/2} = (a^\dagger a)^{1/2}$ is the square root of the photon number operator and ${\rm sinc}(x) = \sin(x)/x$. If the atom–laser coupling is given by (2) with $\delta\tau_L \ll 1$, one finds $\eta\epsilon \simeq \Omega\tan(|\Omega|\tau_L/2)/|\Omega|$. An easy computation using (1) leads to [25]

$$\begin{aligned} {\rm e}^{-{\rm i}\tau H_{\rm int}} &= |g\rangle\langle g|\cos(|\eta| n^{\frac{1}{2}}) + |e\rangle\langle e|\cos(|\eta|(n+1)^{\frac{1}{2}}) \\ &\quad + \eta|e\rangle\langle g|\tilde{a} - \eta^*|g\rangle\langle e|\tilde{a}^\dagger. \end{aligned} \tag{7}$$

Let $|\varphi(t+\delta t)\rangle = \langle j|\Psi_{\rm ent}\rangle$ be the unnormalized wavefunction of the quantum field after the measurement. Since the initial and final atomic states i and j can take two values g or e, we must distinguish four cases.

(1) $i = j = g$. Then, by (3) and (7),

$$\begin{aligned} |\varphi(t+\delta t)\rangle &= u_{gg} W_{g\to g}|\psi(t)\rangle, \\ W_{g\to g} &= \cos(|\eta| n^{\frac{1}{2}}) - |\eta|^2\epsilon^*\tilde{a}. \end{aligned} \tag{8}$$

(2) $i = g$, $j = e$. Then,

$$|\varphi(t+\delta t)\rangle = \eta u_{ee} W_{g\to e}|\psi(t)\rangle,$$
$$W_{g\to e} = W_- \equiv \tilde{a} + \epsilon \cos(|\eta| n^{\frac{1}{2}}). \tag{9}$$

(3) $i = e$, $j = g$. Then,

$$|\varphi(t+\delta t)\rangle = -\eta^* u_{gg} W_{e\to g}|\psi(t)\rangle,$$
$$W_{e\to g} = W_+ \equiv \tilde{a}^\dagger + \epsilon^* \cos(|\eta|(n+1)^{\frac{1}{2}}). \tag{10}$$

(4) $i = j = e$. Then,

$$|\varphi(t+\delta t)\rangle = u_{ee} W_{e\to e}|\psi(t)\rangle,$$
$$W_{e\to e} = \cos(|\eta|(n+1)^{\frac{1}{2}}) - |\eta|^2 \epsilon \tilde{a}^\dagger. \tag{11}$$

Thus, the crossing by the atom of the two cavities and the detector modifies the normalized wavefunction $|\psi(t)\rangle$ of the field in the interaction picture as follows:

$$|\psi(t+\delta t)\rangle = \frac{W_{i\to j}|\psi(t)\rangle}{\|W_{i\to j}|\psi(t)\rangle\|}. \tag{12}$$

The cases (2) and (3) correspond, respectively, to the absorption and the emission of a photon of the quantum field or of the laser field by the atom. We then say that the quantum field suffers a 'quantum jump' − or + (this denomination comes from the limit $|\eta| \to 0$, ϵ fixed, in which these jumps are separated by Hamiltonian-like evolutions [21]). The probability that the atom is detected in state $|j\rangle$, given that it enters the first cavity in state $|i\rangle$, is $p_{i\to j} = \|\langle j|\Psi_{\text{ent}}\rangle\|^2 = \|\varphi(t+\delta t)\|^2$. The probability $\delta p_-(t)$ of a jump − is equal to $p_{g\to e}$ times the probability $r_g \delta t$ that the atom is initially in state $|g\rangle$. Similarly, $\delta p_+(t) = p_{e\to g} r_e \delta t$. Introducing the damping rates

$$\gamma_- = r_g|\eta|^2, \qquad \gamma_+ = r_e|\eta|^2, \qquad \gamma = \gamma_- + \gamma_+ = \frac{|\eta|^2}{\delta t} \tag{13}$$

and using the unitarity of the matrix (u_{ij}), one arrives at

$$\delta p_\pm(t) = \frac{\gamma_\pm \delta t}{1+|\eta\epsilon|^2}\|W_\pm|\psi(t)\rangle\|^2. \tag{14}$$

The probabilities of cases (1) and (4) are respectively $r_g\delta t - \delta p_-(t)$ and $r_e\delta t - \delta p_+(t)$. The stochastic dynamics of the field depends only on the dimensionless parameters η, ϵ and on the damping rates $\gamma_\pm$. The ratio γ_+/γ_- defines the temperature T of the atomic beam:

$$\frac{\gamma_+}{\gamma_-} = \frac{r_e}{r_g} = \exp\left(-\frac{\omega}{k_B T}\right), \tag{15}$$

where ω is the atomic transition frequency and k_B the Boltzmann constant.

4. Localization into squeezed states

Let us follow the evolution of the state $|\psi(t)\rangle$ of the quantum field when many atoms cross the cavities, for a given result (realization) of the measurements. Such a time evolution defines a *quantum trajectory* [3]. We computed $|\psi(t)\rangle$ numerically, taking a particular initial state $|\psi(0)\rangle$ and

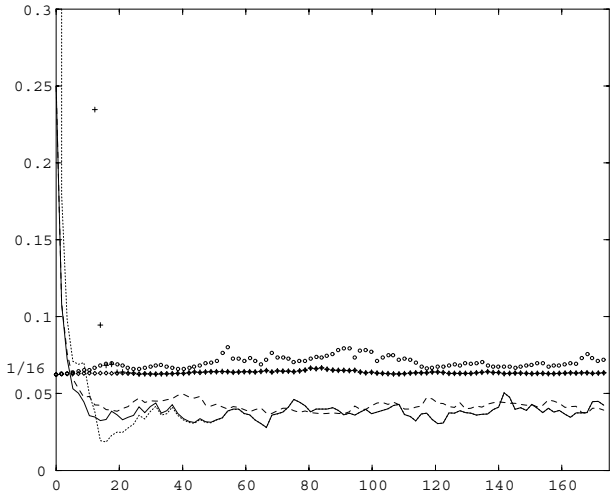

Figure 2. $\Delta x^2(t)$ (full, broken and dotted curves) and $\Delta x^2(t)$ $\Delta y^2(t)$ ($\Diamond$, Oand +) versus γt for three different quantum trajectories. The values of the parameters are $\epsilon = 20$, $\gamma_+/\gamma_- = 3/4$ and $\gamma = 3.5$. The initial state is a coherent state $|\psi(0)\rangle = |\alpha\rangle$ with $\alpha = \sqrt{3/2}(1+\mathrm{i})$ in the trajectory (a) (full curve, $\diamond$) and in the trajectory (b) (broken curve, $\circ$). It is a Fock state $|n\rangle$ with $n = 20$ photons in the trajectory (c) (dotted curve, +). In (a) and (c), the number of atoms crossing the cavity in the whole time interval is $N_A = 5\times10^4$ and $\eta \simeq 0.059$. In (b), $N_A = 5\times10^5$ and $\eta \simeq 0.019$.

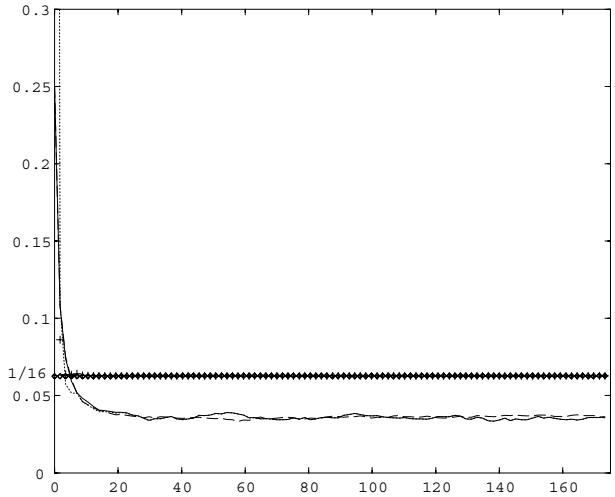

Figure 3. As figure 2, but with $\epsilon = 100$ and with an initial state for the trajectory (c) (dotted curve, +) chosen randomly ($\langle n|\psi(0)\rangle$ is a random number for $0 \leqslant n \leqslant 20$ and vanishes otherwise). For the trajectories (a) and (c) (full and dotted curves, $\diamond$ and +), $N_A = 10^6$ atoms and $\eta \simeq 0.013$. For the trajectory (b) (broken curve, $\circ$), $N_A = 5\times10^6$ and $\eta \simeq 0.006$.

modifying $|\psi(t)\rangle$ according to (12) at each time step δt, with the above probabilities.

For big $|\epsilon|$ and small $|\eta|$, we find that, for any choice of $|\psi(0)\rangle$, $|\psi(t)\rangle$ evolves to a squeezed state $|\alpha(t), \xi(t)\rangle$, up to small fluctuating errors. In order to illustrate this result, let us study the mean square deviations (MSD) $\Delta x_\phi^2(t)$ and $\Delta y_\phi^2(t)$ of the field quadratures $X_\phi = (a\mathrm{e}^{-\mathrm{i}\phi} + a^\dagger \mathrm{e}^{\mathrm{i}\phi})/2$ and $Y_\phi = (a\mathrm{e}^{-\mathrm{i}\phi} - a^\dagger \mathrm{e}^{\mathrm{i}\phi})/2\mathrm{i}$. Denote by $\phi_{\min}(t)$ the angle for which $\Delta x_\phi^2(t) = \langle\psi(t)|X^2_{\phi+\omega t}|\psi(t)\rangle - \langle\psi(t)|X_{\phi+\omega t}|\psi(t)\rangle^2$ is minimum (the phase ωt must be added to ϕ since we are

working in the interaction picture). Let $\Delta x^2(t) = \Delta x^2_{\phi_{\min}(t)}(t)$ and $\Delta y^2(t) = \Delta y^2_{\phi_{\min}(t)}(t)$ be the minimal and maximal MSD. The time evolutions of $\Delta x^2(t)$ and of the product $\Delta x^2(t)\,\Delta y^2(t)$ are shown in figures 2 and 3 for different quantum trajectories. Figure 2 corresponds to $\epsilon = 20$ and figure 3 to $\epsilon = 100$. One sees in both figures that $\Delta x^2(t)$ begins to fluctuate around a mean value $\overline{\Delta x^2}$ after some transient time $\Delta\tau$. The fluctuations are considerably reduced in the case $\epsilon = 100$ (figure 3) with respect to the case $\epsilon = 20$ (figure 2). Moreover, the product $\Delta x^2(t)\,\Delta y^2(t)$ is much closer in figure 3 to the minimum value $1/16$ allowed by Heisenberg's uncertainty principle. The trajectories (a) and (b) start from the same initial coherent state but correspond to different values of η and δt, with fixed damping rate $\gamma = |\eta|^2/\delta t = 7/2$; the trajectory (c) starts from a different initial state (the Fock state in figure 2 and a state chosen by picking the 20 first components $\langle n|\psi(0)\rangle$ randomly in figure 3). The comparison of the different curves, together with other numerical results presented elsewhere [21], indicates that the mean values $\overline{\Delta x^2}$ and $\overline{\Delta x^2\,\Delta y^2} \simeq 1/16$ are independent of:

(1) the specific realization of the measurements;
(2) the initial state $|\psi(0)\rangle$;
(3) the values of ϵ and η, when $|\epsilon|$ is larger than some value ϵ_0 and $|\eta|$ smaller than η_0.

The fact that $\Delta x^2(t)\,\Delta y^2(t)$ fluctuates closer and closer to $1/16$ as $|\epsilon|$ becomes bigger supports the idea that the localization into squeezed states $|\alpha(t), \xi(t)\rangle$ holds in the limit $|\epsilon| \to \infty$. As is well known [22], the minimal MSD of a squeezed state is $\Delta x^2 = \mathrm{e}^{-2|\xi|}/4$. Strikingly, the squeezing amplitude $r(t) = |\xi(t)| = -\ln(2\Delta x(t))$ is nearly deterministic for $t \gtrsim \Delta\tau$, $|\epsilon| \gtrsim \epsilon_0$ and $|\eta| \lesssim \eta_0$, and it depends neither on the initial state nor on η, ϵ. It is important, however, that $|\eta|$ be small enough: for values between 0.06 and 0.09 or greater, we observed completely different behaviours of $\Delta x^2(t)$ and $\Delta x^2(t)\,\Delta y^2(t)$ in figure 2 ($\epsilon = 20$). The same breakdown occurs for $|\eta|$ between 0.02 and 0.04 in figure 3 ($\epsilon = 100$). One can thus expect the localization into squeezed states to be exact in the joint limit $|\epsilon| \to \infty$, $|\eta| \to 0$. The squeezing phase $\phi(t) = \arg(\xi(t))/2$ is also nearly deterministic and is given by $\phi(t) = \arg(\epsilon) - \omega t$ for $t \gtrsim \Delta\tau$ [21]. Unlike $\xi(t)$, the centre $\alpha(t)$ of the squeezed state moves randomly, as seen in figure 4.

Our main result is shown in figure 5. $\Delta x^2(t)$ is plotted versus γt for five quantum trajectories, corresponding to different temperatures T of the atomic beam. It is seen that $\overline{\Delta x^2}$ decreases for increasing T, i.e., the final squeezing increases with the temperature. The purpose of the remaining sections is to explain this phenomenon quantitatively.

5. Photon number statistics

In the absence of measurements, i.e., in the same experimental set-up as in figure 1 but without the detector, the quantum field thermalizes with the atomic beam at temperature $T > 0$. The state of the field is described by a density matrix $\rho(t) = \mathrm{tr}_A\,\sigma(t)$, obtained by tracing out the atomic degrees of freedom in the density matrix $\sigma(t)$ of the total system 'atoms + field'. The probability $\langle n|\rho(t)|n\rangle$ of finding n photons in the first cavity converges at large times to the Bose–Einstein distribution $\rho^{\mathrm{eq}}_{nn} = (1 - \mathrm{e}^{-\omega/k_BT})\mathrm{e}^{-\omega n/k_BT}$. Such a thermalization does not occur if the measurements on the atoms are performed: then the field is constantly maintained out of equilibrium. One should thus keep in mind when confronted with the above-mentioned numerical results that T is the temperature of the atomic beam, not that of the field!

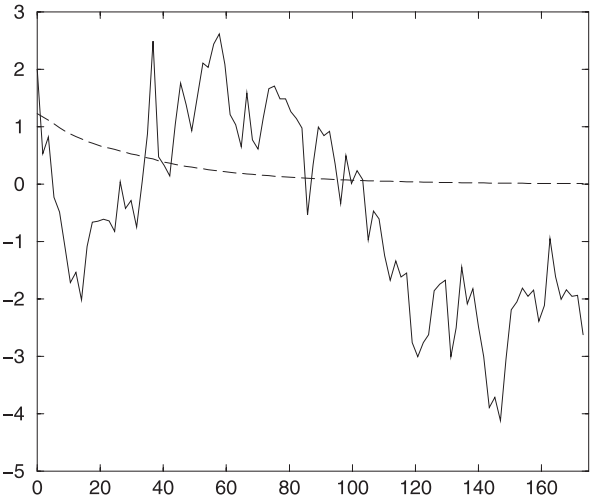

Figure 4. $\mathrm{Re}\langle a\rangle_t$ (full curve) and $\mathrm{Im}\langle a\rangle_t$ (broken curve) versus γt for a quantum trajectory starting from a coherent state $|\psi(0)\rangle = |\alpha\rangle$, with $\gamma_+/\gamma_- = 0.892$, $\gamma = 3.5$, $\eta = 0.0118$, $\epsilon = 84.5 \simeq \eta^{-1}$, $N_A = 1.25 \times 10^6$ atoms and $\alpha = \sqrt{3/2}(1 + \mathrm{i})$.

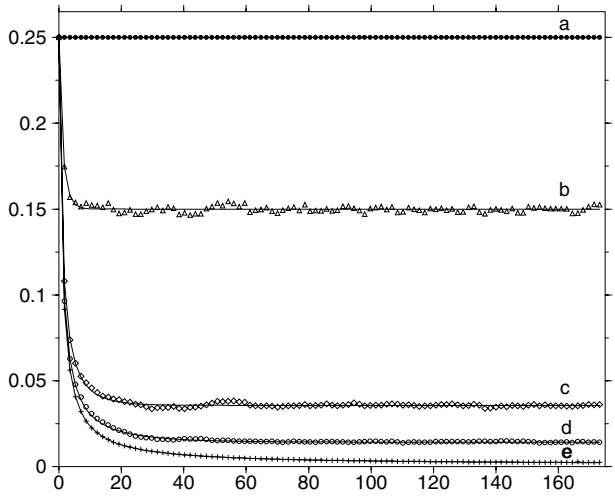

Figure 5. $\Delta x^2(t)$ versus γt for trajectories with different temperatures: (a) $\gamma_+ = 0$, ●; (b) $\gamma_+/\gamma_- = 1/4$, △; (c) $\gamma_+/\gamma_- = 3/4$, ◇; (d) $\gamma_+/\gamma_- = 0.892$, ○; (e) $\gamma_+/\gamma_- = 0.987$, +. In (a), (b) and (c), $\eta = 0.0132$, $N_A = 10^6$ atoms; in (d), $\eta = 0.0118$, $N_A = 1.25 \times 10^6$ atoms; in (e), $\eta = 0.0013$, $N_A = 10^8$ atoms. For all trajectories, $\epsilon = \eta^{-1}$, $\gamma = 3.5$ and the initial coherent state is as in figure 4. The full curves are the theoretical result (39).

Let us denote by M the mean over all results of the measurements. Since averaging the projector $|\psi(t)\rangle\langle\psi(t)|$ over all results of a measurement is the same as not performing the measurement,

$$\rho(t) = \mathrm{tr}_A(\sigma(t)) = \mathsf{M}|\psi(t)\rangle\langle\psi(t)|. \qquad (16)$$

One may verify this formula explicitly by comparing the evolution of the second and third members when one atom

crosses the cavities [21]. It is expected from ergodicity that the time average of the quantum probability $\mathcal{P}_n(t) = |\langle n|\psi(t)\rangle|^2$ of finding n photons coincides with the equilibrium value $\rho_{nn}^{\rm eq}$:

$$\lim_{t\to\infty}\int_0^t \frac{\mathrm{d}s}{t}\,\mathcal{P}_n(t) = \lim_{t\to\infty}\mathsf{M}\mathcal{P}_n(t) = \lim_{t\to\infty}\langle n|\rho(t)|n\rangle = \rho_{nn}^{\rm eq}. \tag{17}$$

In order to check the ergodic hypothesis, we computed numerically the first and fourth members. The corresponding values, represented in figure 6 by the circles and the full curve, agree reasonably well. $\mathcal{P}_n(t)$ is shown in the same figure for a fixed time t. One sees the well known oscillations exhibited by squeezed states, with an overall exponential decay [26]. For squeezed states $|\alpha,\xi\rangle$ with real α and ξ, $\mathcal{P}_n$ has the following asymptotic behaviour as $n\to\infty$:

$$\mathcal{P}_n \sim \frac{2}{\sqrt{\pi}}\left((2n+1)\cosh^2 r - \frac{\mathrm{e}^{2r}\alpha^2}{4\tanh r}\right)^{-\frac{1}{2}} \times \exp\left(\frac{\alpha^2}{2\sinh(2r)}\right)(\tanh r)^n\cos^2(\Phi_n), \tag{18}$$

with $\Phi_n = \int_{\alpha(1-\mathrm{e}^{-4r})^{-1/2}}^{\sqrt{2n+1}}\mathrm{d}x\,\sqrt{2n+1-x^2} - \pi/4$ and $r = |\xi|$ (see [26]). It has been seen in section 4 that the squeezing amplitude $r(t) \simeq -\ln(4\,\overline{\Delta x^2})/2$ is almost time and realization independent for sufficiently large t. This must also be the case for the rate $|\ln(\tanh r)|^{-1}$ of the exponential decay of $\mathcal{P}_n(t)$ as $n\to\infty$. By (17), this rate must coincide with the decay rate k_BT/ω of the Bose–Einstein distribution $\rho_{nn}^{\rm eq}$. This gives $\tanh r = \mathrm{e}^{-\omega/k_BT} = \gamma_+/\gamma_-$. As a result,

$$\overline{\Delta x^2} \simeq \frac{\gamma_- - \gamma_+}{4\gamma} = \frac{1-\mathrm{e}^{-\omega/k_BT}}{4(1+\mathrm{e}^{-\omega/k_BT})}. \tag{19}$$

The values (19) are the large-time limits of the exponentially decaying functions shown in full curves in figure 5. A good agreement is found with the numerical data. Another consequence of (17) is worth noting. In order to reproduce the Bose–Einstein distribution, the oscillations of $\mathcal{P}_n(t)$ as a function of n must disappear after a time (or realization) averaging. Since $|\xi(t)|$ is constant for $t \gtrsim \Delta\tau$, this implies that the centre $\alpha(t)$ of the squeezed state varies randomly in time. The factor $\mathrm{e}^{\alpha^2/2\sinh(2r)}$ in (18) shifts the whole distribution to the right or to the left as α varies, and the amplitude and phase of the oscillations are also changed. These large random time fluctuations are observed for $\mathrm{Re}\,\alpha$ in figure 4.

Formula (19) shows that $\overline{\Delta x^2}$ decreases on increasing T. A perfect squeezing ($\overline{\Delta x^2} = 0$) is predicted at $T=\infty$. However, one finds numerically that the localization into squeezed states only holds for $|\eta|$ smaller than some value η_0 and for $|\epsilon|$ bigger than ϵ_0, where η_0 decreases to zero and ϵ_0 increases to infinity as $k_BT/\omega\to\infty$. Thus perfect squeezing cannot be reached in a practical numerical or real experiment with finite η and ϵ. We shall come back below to this limit of validity of (19).

6. Quantum state diffusion

The argument of section 5 does not explain why the squeezed states form an invariant family under the stochastic dynamics and why the squeezing amplitudes evolve exponentially to a temperature-dependent limiting value at large times, as

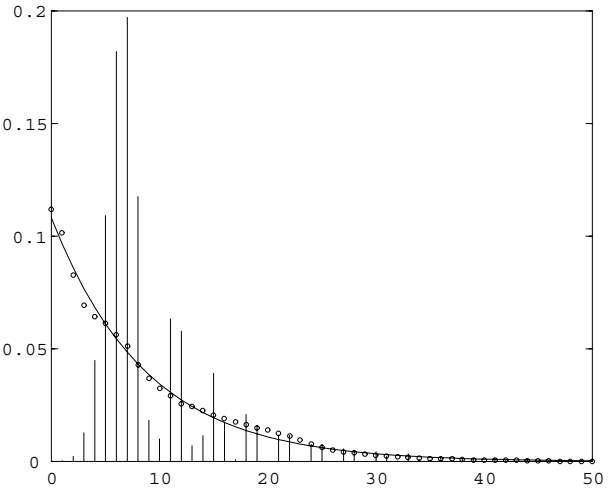

Figure 6. The probability $\mathcal{P}_n(t) = |\langle n|\psi(t)\rangle|^2$ of finding n photons versus n for a given trajectory: (1) at a fixed time $t = 35/\gamma$ (impulses); (2) the time average over 20 000 times in the interval $[10/\gamma, 100/\gamma]$ (circles, ∘). The Bose–Einstein distribution $\rho_{nn}^{\rm eq}$ is shown as a full curve. The parameters are $\gamma_+/\gamma_- \simeq 0.892$, $\epsilon = 100$, $\eta \simeq 0.006$; $\gamma = 3.5$; the initial state is as in figure 4; $N_A = 10^7$ atoms cross the cavity between $t=0$ and $100/\gamma$.

observed in the numerical simulations. In order to understand these points, we determine in this section the coarse-grained evolution of the field state $|\psi(t)\rangle$ for timescales on which many atoms cross the cavities.

The numerical data suggest considering the limit

$$|\epsilon|\to\infty, \qquad |\eta|\to 0, \qquad |\eta\epsilon| = \text{const}. \tag{20}$$

Let us assume moreover that the moments $\langle n^q\rangle_t$ are much smaller than $|\eta|^{-2q}$; more precisely,

$$|\eta|^{2q}\langle n^q\rangle_t = \mathcal{O}(\eta^q), \qquad q = 1,2,\ldots, t \geqslant 0, \tag{21}$$

where $\langle O\rangle_t = \langle\psi(t)|O|\psi(t)\rangle$ is the quantum expectation in state $|\psi(t)\rangle$. Under this condition, the crossing of the cavities and the detector by one atom weakly perturbs the quantum field in all cases (1)–(4) (perturbative regime). In fact, since $|\psi(t)\rangle$ is renormalized at each time step δt, $|\varphi(t+\delta t)\rangle$ is defined up to an arbitrary multiplicative constant in equations (8)–(11). Hence one may divide the right-hand sides of these equations by u_{gg}, $\eta u_{ee}\epsilon$, $-\eta^* u_{gg}\epsilon^*$ and u_{ee}, respectively. This yields

$$|\varphi(t+\delta t)\rangle = (1+\delta W_{i\to j})|\psi(t)\rangle + \mathcal{O}(\eta^{3/2}) \tag{22}$$

with

$$\begin{aligned}
\delta W_{g\to g} &= -\frac{|\eta|^2}{2}(a^\dagger a + 2\epsilon^* a)\\
\delta W_{g\to e} = \delta W_- &= \frac{a}{\epsilon} - \frac{|\eta|^2}{2}a^\dagger a\\
\delta W_{e\to g} = \delta W_+ &= \frac{a^\dagger}{\epsilon^*} - \frac{|\eta|^2}{2}aa^\dagger\\
\delta W_{e\to e} &= -\frac{|\eta|^2}{2}(aa^\dagger + 2\epsilon a^\dagger).
\end{aligned} \tag{23}$$

In all cases (1)–(4), the wavefunction $|\psi(t)\rangle$ is modified by a small amount, of order $\eta^{1/2}$. The equality $\tilde{a} = a + \mathcal{O}(\eta^{1/2})$, which follows from (6) and (21), has been used.

Let us consider a time interval $[t, t+\Delta t]$ such that many atoms cross the cavities between t and $t+\Delta t$ but $|\psi(t+\Delta t)\rangle$ does not differ much from $|\psi(t)\rangle$. This is the case if

$$1 \ll \frac{\Delta t}{\delta t} \ll |\eta|^{-\frac{1}{2}}. \tag{24}$$

Let us denote by $\Delta N_\pm(t)$ the number of jumps $\pm$ (cases (3) or (2)) and by $\Delta N_i(t)$ the number of atoms entering the first cavity in state i ($i = g$ or e) between t and $t+\Delta t$. Then,

$$\begin{aligned}|\varphi(t+\Delta t)\rangle &= [1 + \Delta N_+(t)(\delta W_+ - \delta W_{e\to e}) \\ &\quad + \Delta N_-(t)(\delta W_- - \delta W_{g\to g}) \\ &\quad + \Delta N_e(t)\,\delta W_{e\to e} + \Delta N_g(t)\,\delta W_{g\to g}]|\psi(t)\rangle \\ &\quad + \mathcal{O}\left(\frac{\Delta t}{\delta t}\eta^{\frac{1}{2}}\right)^2. \end{aligned}\tag{25}$$

Since the variation of $|\psi(t)\rangle$ between t and $t+\Delta t$ is small, the jump probability $\delta p_\pm(t_m)$ can be approximated by $\delta p_\pm(t)$ for any $t_m = t + m\delta t$, $m = 0, \ldots, \Delta t/\delta t$. From (9), (10) and (14),

$$\begin{aligned}\mathsf{M}\,\Delta N_\pm(t) &= \sum_{m=0}^{\Delta t/\delta t} \delta p_\pm(t_m) \\ &\simeq \frac{|\epsilon|^2\gamma_\pm\,\Delta t}{1+|\eta\epsilon|^2}\left(1 + \frac{2}{|\epsilon|}\,\mathrm{Re}\langle \mathrm{e}^{-\mathrm{i}\theta}a\rangle_t\right),\end{aligned}$$

with $\epsilon = |\epsilon|\mathrm{e}^{\mathrm{i}\theta}$. Replacing this formula into (25), one obtains the mean value over the measurements of $|\Delta\varphi(t)\rangle = |\varphi(t+\Delta t)\rangle - |\varphi(t)\rangle$:

$$\begin{aligned}\mathsf{M}|\Delta\varphi(t)\rangle &\simeq [2\,\mathrm{Re}\langle \mathrm{e}^{-\mathrm{i}\theta}a\rangle_t(\gamma_+\mathrm{e}^{\mathrm{i}\theta}a^\dagger + \gamma_-\mathrm{e}^{-\mathrm{i}\theta}a)\Delta t \\ &\quad - \tfrac{1}{2}(\gamma_+a^\dagger a + \gamma_-a^\dagger a)\Delta t]|\psi(t)\rangle. \end{aligned}\tag{26}$$

The identity $\mathsf{M}\,\Delta N_i(t) = r_i\,\Delta t$ has been used.

It remains to evaluate the fluctuation of $|\Delta\varphi(t)\rangle$. Consider the random variable $\delta N_i(t_m)$ equal to 1 if the mth atom enters in the first cavity at time $t_m = t + m\,\delta t$ in state $|i\rangle$, and equal to 0 otherwise. The random variable $\delta\tilde N_+(t_m)$ ($\delta\tilde N_-(t_m)$) is equal to 1 if a jump $+$ ($-$) occurs when the mth atom is sent into the cavity in state $|e\rangle$ ($|g\rangle$). The probability that $\delta\tilde N_+(t_m) = 1$ is equal to the conditional probability $p_{e\to g}$ of occurrence of a jump $+$, given that the mth atom is initially in its upper state $|e\rangle$. Similarly, $\delta\tilde N_-(t_m) = 1$ has probability $p_{g\to e}$. Let $i_+ = e$ and $i_- = g$. With these definitions, $\delta N_{i_\pm}(t_m)$ and $\delta\tilde N_\pm(t_m)$ are independent random variables. Variables corresponding to different times t_m are also independent. The fluctuation of $\Delta N_\pm(t) = \sum_{m=0}^{\Delta t/\delta t}\delta N_{i_\pm}(t_m)\,\delta\tilde N_\pm(t_m)$ can be written as a sum of two terms:

$$\begin{aligned}\Delta N_\pm(t) - \mathsf{M}\,\Delta N_\pm(t) &= \sum_{m=0}^{\Delta t/\delta t}\delta N_{i_\pm}(t_m)\,\delta\tilde M_\pm(t_m) \\ &\quad + \sum_{m=0}^{\Delta t/\delta t}\delta M_{i_\pm}(t_m)\,\mathsf{M}\,\delta\tilde N_\pm(t_m),\end{aligned}$$

where $\delta M_i(t_m)$ and $\delta\tilde M_\pm(t_m)$ are the fluctuations of $\delta N_i(t_m)$ and $\delta\tilde N_\pm(t_m)$, respectively. The square variance of the first term is found to be approximately $(\gamma_\pm\Delta t/\gamma\delta t)|\eta\epsilon|^2(1+|\eta\epsilon|^2)^{-2}$. By the central limit theorem,

$$\Delta w_\pm(t) = \sqrt{\frac{\gamma\,\delta t}{\gamma_\pm}}\frac{1+|\eta\epsilon|^2}{|\eta\epsilon|}\sum_{m=0}^{\Delta t/\delta t}\delta N_{i_\pm}(t_m)\,\delta\tilde M_\pm(t_m) \tag{27}$$

tends in the limit $\Delta t \gg \delta t$ to a Gaussian random variable of zero mean and variance Δt. Shifting t by Δt leads to an independent Gaussian variable $\Delta w_\pm(t+\Delta t)$. Hence $\Delta w_\pm(t)$ are the increments of two independent Wiener processes $(w_\pm(t))_{t\geqslant 0}$. With the help of (25), we find

$$\begin{aligned}|\Delta\varphi(t)\rangle - \mathsf{M}|\Delta\varphi(t)\rangle &\simeq \Big[\sqrt{\gamma_+}\mathrm{e}^{\mathrm{i}\theta}a^\dagger\,\Delta w_+(t) \\ &\quad + \sqrt{\gamma_-}\mathrm{e}^{-\mathrm{i}\theta}a\,\Delta w_-(t) + 2|\eta|^2\,\mathrm{Re}\langle \mathrm{e}^{-\mathrm{i}\theta}a\rangle_t \\ &\quad \times (\mathrm{e}^{\mathrm{i}\theta}a^\dagger\Delta M_e(t) + \mathrm{e}^{-\mathrm{i}\theta}a\,\Delta M_g(t)) \\ &\quad - \frac{|\eta|^2}{2}(aa^\dagger\,\Delta M_e(t) + a^\dagger a\,\Delta M_g(t))\Big]|\psi(t)\rangle. \end{aligned}\tag{28}$$

The third and fourth terms, proportional to the fluctuations $\Delta M_i(t)$ of the numbers $\Delta N_i(t)$ of atoms entering the cavity in state i between t and $t+\Delta t$, are of order $(\Delta t/\delta t)^{1/2}\eta$. They can be neglected with respect to the first and second terms, proportional to $\Delta w_\pm(t)$, which are larger by an amount $\eta^{-1/2}$.

Since we are interested in the coarse-grained dynamics of the field with a 'time resolution' Δt, the Gaussian increments $\Delta w_\pm(t)$ will be treated as infinitesimal Itô differentials, denoted by $\mathrm{d}w_\pm(t)$, and Δt will be denoted by a time differential $\mathrm{d}t$.

The last step consists in normalizing $|\varphi(t+\mathrm{d}t)\rangle$. Its inverse norm, assumed to be one at time t, can be computed by using the Itô formalism of stochastic differentials [27]:

$$\begin{aligned}\|\varphi(t+\mathrm{d}t)\|^{-1} &= 1 + \mathrm{d}\left(\frac{1}{\sqrt{\|\varphi(t)\|^2}}\right) \\ &= 1 - \tfrac{1}{2}\,\mathrm{d}\|\varphi(t)\|^2 + \tfrac{3}{8}\,\mathrm{d}\|\varphi(t)\|^2\,\mathrm{d}\|\varphi(t)\|^2. \end{aligned}\tag{29}$$

The first differential in the right-hand side is $\mathrm{d}\|\varphi(t)\|^2 = 2\,\mathrm{Re}\langle\varphi(t)|\mathrm{d}\varphi(t)\rangle + \langle\mathrm{d}\varphi(t)|\mathrm{d}\varphi(t)\rangle$. The last term is non-zero since $\mathrm{d}w_\pm(t)\,\mathrm{d}w_\pm(t) = \mathrm{d}t$. Collecting (26), (28) and (29) and using the other Itô rules $\mathrm{d}w_\pm\,\mathrm{d}w_\mp = \mathrm{d}w_\pm\,\mathrm{d}t = 0$, we arrive at our final result:

$$\begin{aligned}|\mathrm{d}\psi\rangle &= \Big[\sqrt{\gamma_+}(\mathrm{e}^{\mathrm{i}\theta}a^\dagger - \mathrm{Re}\langle\mathrm{e}^{\mathrm{i}\theta}a^\dagger\rangle_t)\,\mathrm{d}w_+(t) \\ &\quad + \sqrt{\gamma_-}(\mathrm{e}^{-\mathrm{i}\theta}a - \mathrm{Re}\langle\mathrm{e}^{-\mathrm{i}\theta}a\rangle_t)\,\mathrm{d}w_-(t) \\ &\quad + \mathrm{Re}\langle\mathrm{e}^{\mathrm{i}\theta}a^\dagger\rangle_t(\gamma_+\mathrm{e}^{\mathrm{i}\theta}a^\dagger + \gamma_-\mathrm{e}^{-\mathrm{i}\theta}a - \frac{\gamma}{2}\,\mathrm{Re}\langle\mathrm{e}^{\mathrm{i}\theta}a^\dagger\rangle_t)\,\mathrm{d}t \\ &\quad - \tfrac{1}{2}(\gamma_+aa^\dagger + \gamma_-a^\dagger a)\,\mathrm{d}t\Big]|\psi(t)\rangle. \end{aligned}\tag{30}$$

Note that $|\mathrm{d}\psi\rangle$ is independent of $|\eta\epsilon|$, i.e., the coarse-grained dynamics depends only on $\theta = \arg\epsilon$ and on the damping constants γ_+ and γ_-.

Equation (30) pertains to a known class of stochastic Schrödinger equations with real Wiener processes, which has been studied in [8, 10]; related equations with complex Wiener processes have been discussed in [9]. Both kinds of equation unravel the same Lindblad master equation for the density matrix (16). In our case, the master equation is easy to determine directly. The change of $\rho(t)$ when one atom, initially in state $|i\rangle$, crosses the cavity is

$$\rho(t+\delta t) = \mathrm{tr}_A(\mathrm{e}^{-\mathrm{i}\tau H_{\mathrm{int}}}|i\rangle\langle i|\rho(t)\mathrm{e}^{\mathrm{i}\tau H_{\mathrm{int}}}). \tag{31}$$

$\rho(t)$ describes the evolution of the quantum field without the measurements on the atoms. Hence it does not depend upon the classical field $\mathcal{E}$ in the second cavity (this is seen

mathematically by using the cyclicity of the trace to get rid in (31) of the two exponentials $e^{\pm i\tau_L H_L}$ multiplying $e^{\pm i\tau H_{\rm int}}$). The coarse-grained average dynamics on the timescale $\Delta t \gg \delta t$ is obtained by replacing (7) into (31), using similar approximations to those above. Not surprisingly, one finds the equation of the damped harmonic oscillator:

$$\frac{d\rho}{dt} = \gamma_-\big(a\rho(t)a^\dagger - \tfrac{1}{2}\{a^\dagger a, \rho(t)\}\big) + \gamma_+\big(a^\dagger\rho(t)a - \tfrac{1}{2}\{aa^\dagger, \rho(t)\}\big). \quad (32)$$

The curly brackets denote the anticommutators. Although the quantum trajectories depend on $\arg(\epsilon)$, the corresponding master equation is the same for all ϵs. The equilibrium is the Bose–Einstein matrix $\rho^{\rm eq}$ with temperature T ($T \geqslant 0$).

Let us end this section by making two remarks. Firstly, the above analysis can be carried out under the following hypothesis, which is more general than (21):

$$\langle(|\eta|n^{\frac{1}{2}} - k\pi)^{2q}\rangle_t = \mathcal{O}(\eta^q), \qquad q = 1, 2, \ldots, t \geqslant 0, \quad (33)$$

with k a non-negative integer. For $k \geqslant 1$, this means that the typical number of photons is close to $(k\pi/|\eta|)^2 \gg 1$, with relative fluctuations at most of order $|\eta|$. Then, most atoms crossing the first cavity make approximately $k/2$ Rabi oscillations and leave it almost in the same state as when they entered it. The coarse-grained stochastic and average dynamics are then given by (30) and (32) with a replaced by $\tilde{a}$ and θ replaced by $\theta + k\pi$. If $(k\pi/|\eta|)^2$ is an integer n_k, $\tilde{a}^\dagger|n_k - 1\rangle = 0$ and the atoms cannot bring more than $n_k - 1$ photons into the cavity (trapping states) [15]. Secondly, let us mention that the stochastic dynamics of section 3 has been studied in [21] in the limit $|\eta| \to 0$, keeping ϵ finite and assuming that (21) holds. This yields a quantum jump (or Monte Carlo wavefunction) model similar to the model introduced in [2, 3]. This is because for small $|\eta\epsilon|$ and $|\eta|$, the jump probabilities $\delta p_\pm(t)$ are very small (see (14)) and the (coarse-grained) evolution between these jumps is Hamiltonian-like, with an effective non-self-adjoint Hamiltonian $K = \gamma_-(a^\dagger a + 2\epsilon^* a + |\epsilon|^2)/2i + \gamma_+(aa^\dagger + 2\epsilon a^\dagger + |\epsilon|^2)/2i$. The jump operators are $W_- = a + \epsilon$ and $W_+ = a^\dagger + \epsilon^*$. Both K and $W_\pm$ depend on ϵ. The limit $|\epsilon| \to \infty$ of the quantum jump dynamics of course gives the stochastic Schrödinger equation (30) again [6, 21].

7. Evolution of the squeezing parameters

As shown by Rigo and Gisin [28], the stochastic Schrödinger equation (30) preserves squeezed states. More precisely, $|\psi(t)\rangle = |\alpha(t), \xi(t)\rangle$ is a solution of (30) if $\alpha(t)$ and $\xi(t) = r(t)e^{2i\phi(t)}$ satisfy the Itô stochastic differential equations:

$$\begin{aligned} d\Gamma &= -e^{2i\theta}(1 + e^{-2i\theta}\Gamma(t))(\gamma_+ + \gamma_- e^{-2i\theta}\Gamma(t))\,dt \\ d\beta &= -\left(\frac{\gamma}{2} + \gamma_- e^{-2i\theta}\Gamma(t)\right)\beta(t)\,dt \\ &\quad + 2(\gamma_+ e^{i\theta} + \gamma_- e^{-i\theta}\Gamma(t))\,\mathrm{Re}(e^{-i\theta}\alpha(t))\,dt \\ &\quad + \sqrt{\gamma_+}e^{i\theta}\,dw_+(t) + \sqrt{\gamma_-}e^{-i\theta}\Gamma(t)\,dw_-(t), \end{aligned} \quad (34)$$

with $\Gamma(t) = -e^{2i\phi(t)}\tanh(r(t))$ and $\beta(t) = \alpha(t) - \Gamma(t)\alpha^*(t)$. These equations are derived in [21, 28], so we only quote here the result (note that $dw_\pm$ are Itô stochastic differentials, whereas Stratanovich differentials are used in [28]). The squeezing parameters $r(t)$ and $\phi(t)$ are given by the solution of the first equation, which is deterministic:

$$-\Gamma(t) = e^{2i\phi(t)}\tanh(r(t)) = e^{2i\theta}\frac{\gamma_+ e^{(\gamma_- - \gamma_+)t} + c}{\gamma_- e^{(\gamma_- - \gamma_+)t} + c}, \quad (35)$$

where c is an arbitrary complex constant. Replacing (35) into the second equation in (34), $x_\theta(t) = \mathrm{Re}(e^{-i\theta}\alpha(t))$ and $y_\theta(t) = \mathrm{Im}(e^{-i\theta}\alpha(t))$ are found to satisfy

$$\begin{aligned} dx_\theta &= -\frac{\gamma_- - \gamma_+}{2}x_\theta(t)\,dt + \frac{\gamma_- e^{(\gamma_- - \gamma_+)t} + c}{\gamma e^{(\gamma_- - \gamma_+)t} + 2c}\sqrt{\gamma_+}\,dw_+(t) \\ &\quad - \frac{\gamma_+ e^{(\gamma_- - \gamma_+)t} + c}{\gamma e^{(\gamma_- - \gamma_+)t} + 2c}\sqrt{\gamma_-}\,dw_-(t) \\ dy_\theta &= -\frac{\gamma_- - \gamma_+}{2}y_\theta(t)\,dt. \end{aligned} \quad (36)$$

The second equation is again deterministic and gives

$$y_\theta(t) = \mathrm{Im}(e^{-i\theta}\alpha(t)) = e^{-(\gamma_- - \gamma_+)t/2}y_\theta(0). \quad (37)$$

In figure 4, we indeed observe an exponential decay of $y_0(t) = \mathrm{Im}\langle a\rangle_t$ with the rate $(\gamma_- - \gamma_+)/2$.

In the large-time limit $t \gg (\gamma_- - \gamma_+)^{-1}$, the centre $\alpha(t)$ moves randomly on the line $\arg(\alpha) = \theta$, and

$$\tanh(r(t)) \to \frac{\gamma_+}{\gamma_-} = \exp\left(-\frac{\omega}{k_B T}\right), \qquad \phi(t) \to \theta. \quad (38)$$

Since for squeezed states $\Delta x^2 = e^{-2r}/4$, one recovers the expression (19) for the time average (or, equivalently, the infinite-time limit) of $\Delta x^2(t)$. In the Schrödinger picture, the field wavefunction is $|\psi_S(t)\rangle = |\alpha(t)e^{-i\omega t}, \xi(t)e^{-2i\omega t}\rangle$. The centre of this squeezed state now also rotates in the complex plane. The squeezing phase is $\phi_S(t) \simeq \theta - \omega t$ at large times.

In the special case of an initial coherent state $|\psi(0)\rangle = |\alpha\rangle$, the constant c is equal to $-\gamma_+$, so $\phi(t) = \theta$ at all times and

$$\Delta x^2(t) = \frac{\gamma_- - \gamma_+}{4\gamma_- + 4\gamma_+(1 - 2e^{-(\gamma_- - \gamma_+)t})}. \quad (39)$$

In particular, $\Delta x^2(t) = 1/4$ at zero temperature ($\gamma_+ = 0$). This means that coherent states $|\psi(t)\rangle = |\alpha(t)\rangle$ are preserved by the stochastic dynamics if all atoms are initially in their lower state. The result (39) is compared in figure 5 with the numerical data. One sees a very good agreement. Note that the rate $(\gamma_- - \gamma_+)$ of the exponential decay of $\Delta x^2(t)$ decreases to zero at high temperatures: one needs to wait longer and longer to reach the value $\overline{\Delta x^2}$ given by (19) as T becomes larger. In any real or numerical experiment, the quantum field is observed up to a finite time t, so this limits the maximal squeezing that can be reached: $\Delta x^2(t) > \overline{\Delta x^2}$.

By ergodicity, the time average of $\langle n\rangle_t$ is the Bose–Einstein average $1/(e^{\omega/k_B T} - 1)$. For squeezed states, $\langle n\rangle = \sinh^2 r + |\alpha|^2$ (see [22]). Using (38) gives the time average of $|\alpha(t)|^2$:

$$\overline{|\alpha|^2} = \overline{x_\theta^2} = \frac{\gamma_+\gamma_-}{\gamma(\gamma_- - \gamma_+)}. \quad (40)$$

8. Limitations on the squeezing

Let us discuss the limit of validity of (19) and (39). The first restriction comes from the fact that real cavities are not perfect. In experiments with micromasers [15], the time δt separating consecutive atoms is smaller than the photon lifetime $t_{\rm cav}$ and the interaction time τ is small compared with δt, in order to avoid events involving more than one atom in the cavity. It is legitimate under these conditions to neglect photon losses during the interaction. The dynamics thus splits into squeezing and damping cycles, with time durations τ and $\delta t - \tau$, respectively. In order to ensure that damping cycles do not destroy the squeezing effect, $\gamma t_{\rm cav}$ must be large enough. The interesting problem of the determination of the large-time limit of the field state in the presence of photon losses is left to a future work. Note also that the presence of thermal photons in the cavity has not been taken into account in our analysis. These can be neglected if the cavity is cooled at very low temperature (much smaller than the temperature T of the beam), as is generally the case in the experiments [15].

A second limitation is brought about by the fact that the computation of section 6 and the preservation of squeezed states by the dynamics is only valid in the limits (20) and (21). A closer look at (23) shows that the condition of validity is

$$|\eta|^2|\epsilon|\sqrt{\langle n\rangle_t} \ll 1 \qquad \text{and} \qquad |\epsilon|^{-1}\sqrt{\langle n\rangle_t} \ll 1 \tag{41}$$

at all times. Given η and T, the best choice of $|\epsilon|$ minimizing both quantities in (41) is clearly $|\epsilon| = |\eta|^{-1}$. Then the condition reduces to $|\eta|\langle n\rangle_t^{1/2} \ll 1$. At low or intermediate temperatures, the mean number of photons in the cavity is not very large and this condition is met in the weak-coupling limit $|\eta| = |\lambda|\tau \ll 1$.

However, since $\overline{\langle n\rangle} = 1/(\mathrm{e}^{\omega/k_BT} - 1)$ increases to infinity at large T, the condition (41) is violated, for any value of η, above a certain temperature T_0 depending on η and ϵ. For $T \gtrsim T_0$, the localization of the quantum field into squeezed states no longer occurs. This reasoning explains qualitatively why we had to go to smaller values of η and higher values of ϵ when increasing T in the simulations of figure 5. Taking $|\epsilon| = |\eta|^{-1}$, $k_BT_0/\omega \simeq \gamma_+(\gamma_- - \gamma_+)^{-1}$ must be small with respect to $|\eta|^{-2}$. This gives, however, an overestimation of T_0, since the fluctuations of $\langle n\rangle_t = \sinh^2 r + |\alpha(t)|^2$, which appear to be important in figure 4, have not been taken into account.

One may be concerned that, even if (41) is fulfilled, the error made after $N_A \gg 1$ atoms have crossed the cavity might be large, despite the smallness of the error made for each atom taken separately. We argue below that such an accumulation of errors at large times, if it exists, leads to much smaller errors than one might expect. It seems reasonable to assume that only the average part of the variation of the state $|\psi(t)\rangle$ when one atom crosses the cavities, denoted by $\mathsf{M}_t|\delta\psi(t)\rangle$, can lead to accumulating errors. For fixed $|\psi(t)\rangle = |\alpha, \xi\rangle$ and $|\epsilon| = |\eta|^{-1}$,

$$|\psi(t)\rangle + \mathsf{M}_t|\delta\psi(t)\rangle = |\alpha + \delta\alpha, \xi + \delta\xi\rangle + \mathcal{O}(\eta^4\langle n\rangle_t^2). \tag{42}$$

The proof of this formula is based on the following result: if b, $c_\pm$ and d are complex numbers with $b = 1 + \mathcal{O}(\eta)$, $c_\pm = \mathcal{O}(\eta^2\sqrt{\langle n\rangle_t})$ and $d = \mathcal{O}(\eta^2)$, then there are complex numbers α' and ξ' and a normalization constant A such that

$$(b + c_+a^\dagger + c_-a + dn)|\alpha, \xi\rangle = A|\alpha', \xi'\rangle + \mathcal{O}(\eta^4\langle n\rangle_t^2). \tag{43}$$

Indeed, using the known properties of squeezed states, this is equivalent to the existence of an operator $(a - \Gamma' a^\dagger - \beta')$, with Γ' and $\beta' \in \mathbb{C}$, which, when applied to the left-hand member of (43), gives zero plus some terms of order $\eta^4\langle n\rangle_t^2$. A simple computation shows that such Γ' and β' exist. This proves (43). The mean variation $\mathsf{M}_t|\delta\varphi(t)\rangle$ of the unnormalized wavefunction $|\varphi(t)\rangle$ is given, to lowest order, by (26) with $\Delta t = \delta t$. It can be further checked that it has the same form as the left-hand member of (43), with $b, c_\pm$ and d satisfying the above hypothesis, up to corrections of order $\eta^4\langle n\rangle_t^2$. Moreover, as is clear from (22) and (23), the fluctuation $|\delta\varphi_f(t)\rangle = (1-\mathsf{M}_t)|\delta\varphi(t)\rangle$ is also of the form (43), up to terms of order $\eta^3\langle n\rangle_t^{3/2}$, but with $b, d = \mathcal{O}(\eta^2)$ and $c_\pm = \mathcal{O}(\eta)$. We now write

$$\begin{aligned}|\psi(t)\rangle + \mathsf{M}_t|\delta\psi(t)\rangle &= C(|\psi(t)\rangle + \mathsf{M}_t|\delta\varphi(t)\rangle)\\ &\quad + \mathsf{M}_t(\|\varphi(t+\delta t)\|^{-1} - 1)|\delta\varphi_f(t)\rangle,\end{aligned}$$

with $C = \mathsf{M}_t\|\varphi(t+\delta t)\|^{-1}$. Since $|\delta\varphi_f(t)\rangle = \mathcal{O}(\eta\sqrt{\langle n\rangle_t})$, this makes it clear that $|\psi(t)\rangle + \mathsf{M}_t|\delta\psi(t)\rangle$ is also of the form (43) with $b, c_\pm$ and d satisfying the above hypothesis. It follows that (42) holds true.

Let us assume that the above errors accumulate. The total error after the crossing of a large number N_A of atoms is then

$$\sum_{m=0}^{N_A}|\eta|^4\langle n\rangle_{m\,\delta t}^2 \simeq N_A|\eta|^4\overline{\langle n\rangle_t^2} \leqslant N_A|\eta|^4\overline{\langle n^2\rangle_t} = \frac{\gamma_+\gamma N_A|\eta|^4}{(\gamma_- - \gamma_+)^2}, \tag{44}$$

where the last expression is the average of n^2 at thermal equilibrium. If N_A is bigger than $(N_A)_0 = |\eta|^{-4}(\gamma_- - \gamma_+)^2/\gamma_+\gamma$, or, equivalently, if γt is bigger than

$$\gamma t_0 = \frac{(\gamma_- - \gamma_+)^2}{\gamma_+\gamma|\eta|^2}, \tag{45}$$

then the field state should differ significantly from a squeezed state. Replacing the values of γ_+ and γ_- in the trajectories (d) and (e) in figure 5, one finds $\gamma t_0 \simeq 50$. Nevertheless, a good agreement with (39) is observed at much bigger times! Numerically, we find that $\Delta x^2(t)\,\Delta y^2(t)$ cannot be distinguished from $1/16$ over the whole time interval, using the scale of figure 5. The values of γt_0 for the trajectories (a), (b) and (c) are higher; other simulations not presented here also show no deviation of $\Delta x^2(t)\,\Delta y^2(t)$ from $1/16$ for e.g. $\gamma_-/\gamma_+ = 3/4$ and $\eta = \epsilon^{-1} = 0.03$, corresponding to $\gamma t_0 \simeq 50$ (but the fluctuations of $\Delta x^2(t)$ around $(\gamma_- - \gamma_+)/4\gamma$ have a larger amplitude). Moreover, longer-time simulations, running up to $t = 1750/\gamma$, show no further deviations of the quantum field from a squeezed state, and the squeezing amplitudes continue to fluctuate around the value (39). Hence one can conclude that there are no accumulations of errors of the kind studied above.

9. Conclusions

We have presented a quantum trajectory model applied to a particularly simple optical system, that of a damped harmonic oscillator at temperature T. The model that we have considered is a beam of two-level atoms crossing one by one a lossless cavity containing the quantum field studied, coupled to a classical field and finally to a detector at the exit of the cavity.

The idealized case of two-level atoms interacting with a single mode of the electromagnetic field in a lossless cavity is nearly realized in micromasers [15]. In the recent experiment [29], a cavity with a quality factor as high as $Q = 4 \times 10^{10}$ has been employed, corresponding to a photon lifetime $t_{\rm cav} = 0.3$ s. The main difference between the physics of the micromaser and our model is that, in the experiments known to us, the two-level atoms are pumped in their upper level before interacting with the quantum field, whereas we assumed in this work that the atomic beam has a positive temperature T. We have given numerical evidence that, for a non-zero classical field intensity and a small enough coupling strength $\eta = \lambda\tau$ (λ is the atom–field coupling constant and τ the time spent by each atom in the cavity), the cavity field localizes into squeezed states. The corresponding squeezing amplitude $r(t)$ and phase $\phi(t)$ have been shown to be nearly deterministic and given by (38) in the large-time limit. The centre $\alpha(t)$ of the squeezed state moves randomly in the complex plane, in such a way that the quantum probabilities for the photon numbers reproduce the thermal (Bose–Einstein) distribution after a time averaging. The main result is that the final degree of squeezing increases with the temperature of the atomic beam. A perfect squeezing can be obtained *a priori* in the limit of infinite tempeature and of zero coupling strength η, keeping a finite laser field intensity. However, the time needed to obtain this perfect squeezing goes to infinity in this high-temperature limit, and corrections for finite η and ϵ become important at high temperatures. This, together with the finite lifetime of photons in a real cavity, limits in practice the squeezing that can be achieved.

The squeezing effect found in the present work should be in principle observable in micromasers. Since the probability of field-induced transitions between adjacent atomic levels with principal quantum number n scales as n^4, experiments with values of η ranging from 10^{-3} to more than 1 can be found in the literature. According to our numerical simulations, the best value for observing a rapid localization of the cavity field into squeezed states is $\eta \simeq 0.03$, and the localization time is typically $t \simeq 10/\gamma$ with $\gamma = \eta^2\,\delta t^{-1}$. The experiments described in [15] have higher values of η, due to the high degree of excitation of the rubidium atoms ($\lambda = 10^4$ s^{-1} for the $63p_{3/2} \rightarrow 61d_{3/2}$ transition and the shorter τ is 25×10^{-6} s, giving $\eta = 0.25$). The intensity of the beam must be small enough in order to ensure that the cavity field is coupled to at most one atom at any time. Using a flux of atoms $r = \delta t^{-1} = 0.1\tau^{-1}$, one finds, assuming a Poissonian statistics for the number of atoms in the cavity, that 95% of the events involve only one atom. This flux is in the range of the experimental data for $\tau = 25 \times 10^{-6}$ s. The condition of observation of the predicted localization into squeezed states is met for $\gamma t_{\rm cav} = \eta^2 t_{\rm cav}(0.1\tau^{-1}) \gtrsim 10$ and $\eta \lesssim 0.03$. One concludes that τ must be smaller than 3×10^{-6} s. Again, this value is a bit too small compared with typical micromaser experimental data (relatively large cavities are used in order to ensure that the low mode is in resonance with the nearby Rydberg level transition). In order to observe the temperature-enhanced squeezing described in this work, atomic transitions corresponding to lower coupling constants could be more suitable, or faster atoms spending less time in the cavity could be used. According to [15], the squeezing of the cavity field could be measured by using probe atoms.

Acknowledgments

DS is grateful to Walter Strunz for fruitful discussions. DS acknowledges the financial support during the early stages of this work of a Fondecyt postdoctoral grant 3000035. MO acknowledges the financial support of the Fondecyt project 1010777.

References

[1] Carmichael H, Singh S, Ryas R and Rice P R 1989 *Phys. Rev.* A **39** 1200
[2] Dalibard J, Castin Y and Mølmer K 1992 *Phys. Rev. Lett.* **68** 580
Mølmer K, Castin Y and Dalibard J 1993 *J. Opt. Soc. Am.* B **10** 524
[3] Carmichael H 1991 *An Open System Approach to Quantum Optics (Springer Lecture Notes in Physics vol 18)* (Berlin: Springer)
[4] Hegerfeldt G C and Wilser T S 1993 *Proc. 2nd Int. Wigner Symp. (Goslar, July 1991)* ed H D Doelner, W Scherer and F Schroeck (Singapore: World Scientific)
[5] Gardiner C W, Parkins A S and Zoller P 1992 *Phys. Rev.* A **46** 4363
[6] Wiseman H M and Milburn G J 1993 *Phys. Rev.* A **47** 642
[7] Plenio M B and Knight P L 1998 *Rev. Mod. Phys.* **70** 101
[8] Gisin N 1984 *Phys. Rev. Lett.* **52** 1657
and see also
Diósi L 1988 *Phys. Lett.* A **129** 419
[9] Gisin N and Percival I C 1992 *J. Phys. A: Math. Gen.* **25** 5677
[10] Ghirardi G C, Pearle P and Rimini A 1990 *Phys. Rev.* A **42** 78
[11] Belavkin V P 1990 *J. Math. Phys.* **31** 2930
Barchielli A and Belavkin V P 1991 *J. Phys. A: Math. Gen.* **24** 1495
[12] Spehner D and Bellissard J 2001 *J. Stat. Phys.* **104** 525
Spehner D and Bellissard J 2001 *Modern Challenges in Quantum Optics (Springer Lecture Notes in Physics vol 575)* ed M Orszag and J C Retamal (Berlin: Springer)
[13] Brune M, Haroche S, Lefevre V, Raimond J M and Zagury N 1990 *Phys. Rev. Lett.* **65** 976
Brune M, Haroche S, Raimond J M, Davidovich L and Zagury N 1992 *Phys. Rev.* A **45** 5193
Wunderlich C, Raimond J M and Haroche S 1996 *Phys. Rev. Lett.* **77** 4887
[14] Meschede D, Walther H and Müller G 1985 *Phys. Rev. Lett.* **54** 551
[15] Raithel G, Wagner C, Walther H, Narducci L M and Scully M O 1994 *Cavity Quantum Electrodynamics* ed P R Berman (Boston, MA: Academic) p 57
[16] An K, Childs J J, Dasari R R and Feld M 1994 *Phys. Rev. Lett.* **73** 3375
[17] Neuhauser W, Dehmelt H G and Toschek P E 1980 *Phys. Rev.* A **22** 1137
Nagourney W, Sandberg J and Dehmelt H G 1986 *Phys. Rev. Lett.* **56** 2797
Sauter T, Neuhauser W, Blatt R and Toschek P E 1986 *Phys. Rev. Lett.* **57** 1696
Bergquist J C, Hulet R G, Itano W M and Wineland D J 1986 *Phys. Rev. Lett.* **57** 1699
Dietrich F, Bergquist J C, Itano W M and Wineland D J 1989 *Phys. Rev. Lett.* **62** 403
[18] Ralph D C, Black C T and Tinkham M 1997 *Phys. Rev. Lett.* **78** 4087
[19] Andrews M R, Townsend C J, Miesner H J, Durfee D S, Kurn D M and Ketterle W 1997 *Science* **275** 637
[20] Wellens T, Buchleitner A, Kümmerer B and Maasen H 2000 *Phys. Rev. Lett.* **85** 3361

[21] Spehner D and Orszag M 2002 *J. Math. Phys.* **43** 3511
[22] Orszag M 2000 *Quantum Optics* (Berlin: Springer)
[23] Kist T B L, Orszag M, Brun T A and Davidovich L 1999 *J. Opt. B: Quantum Semiclass. Opt.* **1** 251
[24] Wagner C, Brecha R J, Schenzle A and Walther H 1992 *Phys. Rev.* A **46** R5350
Englert B-G, Gantsog T, Schenzle A, Wagner C and Walther H 1996 *Phys. Rev.* A **53** 4386
[25] Stenholm S 1973 *Phys. Rep.* C **6** 1
[26] Schleich W and Wheeler J A 1991 *Non-Classical Effects in Quantum Optics* ed P Meystre and D F Walls (New York: AIP)
[27] Gardiner C W 1983 *Handbook of Stochastic Methods for Physics, Chemistry and the Natural Sciences* (Berlin: Springer)
[28] Rigo M and Gisin N 1996 *Quantum Semiclass. Opt.* **8** 255
[29] Brattke S, Varcoe B T H and Walther H 2001 *Phys. Rev. Lett.* **86** 3534